Exploring chemical versatility within the tautomerase superfamily

Baas, Jan

Chapter 2

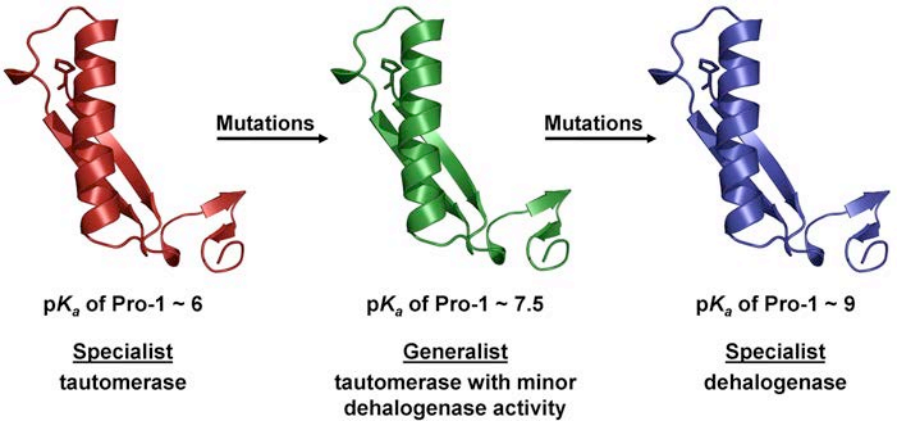

Characterization of a newly identified Mycobacterial tautomerase with promiscuous dehalogenase and hydratase activities reveals a functional link to a recently diverged *cis*-3-chloroacrylic acid dehalogenase.

Bert-Jan Baas, Ellen Zandvoort, Anna A. Wasiel, Wim J. Quax, and Gerrit J. Poelarends

Department of Pharmaceutical Biology, Groningen Research Institute of Pharmacy, University of Groningen, Antonius Deusinglaan 1, 9713 AV Groningen, The Netherlands

Published in *Biochemistry* (2011) 50, 2889-2899.

Abstract

The enzyme *cis*-3-chloroacrylic acid dehalogenase (*cis*-CaaD) is found in a bacterial pathway that degrades a synthetic nematocide, *cis*-1,3-dichloropropene, introduced in the 20th century. The previously determined crystal structure of *cis*-CaaD and its promiscuous phenylpyruvate tautomerase (PPT) activity link this dehalogenase to the tautomerase superfamily, a group of homologous proteins that are characterized by a catalytic amino-terminal proline and a β-α-β structural fold. The low-level PPT activity of *cis*-CaaD, which may be a vestige of the function of its progenitor, prompted us to search the databases for a homologue of *cis*-CaaD that was annotated as a putative tautomerase and test both its PPT and *cis*-CaaD activity. We identified a mycobacterial *cis*-CaaD homologue (designated MsCCH2) that shares key sequence and active site features with *cis*-CaaD. Kinetic and ^{1}H NMR spectroscopic studies show that MsCCH2 functions as an efficient PPT and exhibits low-level promiscuous dehalogenase activity, processing both *cis*- and *trans*-3-chloroacrylic acid. To further probe the active site of MsCCH2, the enzyme was incubated with 2-oxo-3-pentynoate (2-OP). At pH 8.5, MsCCH2 is inactivated by 2-OP due to the covalent modification of Pro-1, suggesting that Pro-1 functions as a nucleophile at pH 8.5 and attacks 2-OP in a Michael-type reaction. At pH 6.5, however, MsCCH2 exhibits hydratase activity and converts 2-OP to acetopyruvate, which implies that Pro-1 is cationic at pH 6.5 and not functioning as a nucleophile. At pH 7.5, the hydratase and inactivation reactions occur simultaneously. From these results, it can be inferred that Pro-1 of MsCCH2 has a pK_a value that lies in between that of a typical tautomerase (pK_a of Pro-1 ~6) and that of *cis*-CaaD (pK_a of Pro-1 ~9). The shared activities and structural features, coupled with the intermediate pK_a of Pro-1, suggest that MsCCH2 could be characteristic of an evolutionary intermediate along the past route for the divergence of *cis*-CaaD from an unknown superfamily tautomerase. This makes MsCCH2 an ideal candidate for laboratory evolution of its promiscuous dehalogenase activity, which could identify additional features necessary for a fully active *cis*-CaaD. Such results will provide insight into pathways that could lead to the rapid divergent evolution of an efficient *cis*-CaaD enzyme.

Introduction

The bacterial enzymes *trans*-3-chloroacrylic acid dehalogenase (CaaD)[1] and *cis*-3-chloroacrylic acid dehalogenase (*cis*-CaaD) catalyze the hydrolytic dehalogenation of the *trans*- and *cis*-isomers of 3-chloroacrylate (**2** and **3**, respectively) to yield malonate semialdehyde (**4**) and HCl (Scheme 1) (*1-3*). These reactions represent key steps in the degradation of the synthetic nematocide 1,3-dichloropropene (**1**), which was introduced into the environment in the 20th century (*4*,*5*). Both dehalogenases belong to the tautomerase superfamily and as such share a β-α-β structural fold and a catalytic amino-terminal proline (*6-8*). However, they are not members of the same family and likely have evolved independently from respective family progenitors (*3,8*). This is quite surprising given the fact that CaaD and *cis*-CaaD use similar catalytic mechanisms to process the different isomers of 3-chloroacrylate (*9-14*). Despite their most recent emergence, the evolutionary origins of CaaD and *cis*-CaaD remain elusive.

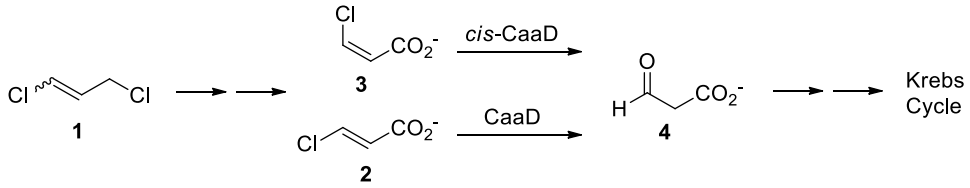

Scheme 1.

CaaD is a heterohexamer consisting of three α-subunits (75 amino acid residues each) and three β-subunits (70 amino acid residues each) (*1*). Similarities in sequence and tertiary and quaternary structures connect CaaD to members of the 4-oxalocrotonate tautomerase (4-OT) family within the tautomerase superfamily (*1,9,15*). 4-OT is part of a bacterial degradation pathway for aromatic hydrocarbons such as toluene (**5**) and converts 2-hydroxy-2,4-hexadienedioate (**6**) to 2-oxo-3-hexenedioate (**7**) (Scheme 2) (*15-19*). The evolutionary link between CaaD and members of the 4-OT family is strengthened by the observations that 4-OT from *Pseudomonas putida* mt-2 and YwhB, a 4-OT homologue from *Bacillus subtilis*, show low-level CaaD activity (*20*). This suggests that a 4-OT-like enzyme could have been recruited to serve as a CaaD because it fortuitously had a low but useful level of dehalogenase activity (*7,20*). Indeed, CaaD exhibits vestigial tautomerase activity and, like 4-OT and YwhB, converts phenylenolpyruvate (**8**) to phenylpyruvate (**9**) (Scheme 3) (*21*).

cis-CaaD, a trimer composed of three identical monomers (149 amino acid residues each), is the title enzyme of a separate family within the tautomerase superfamily (*3*). This dehalogenase also exhibits vestigial tautomerase activity, albeit at a low-level, converting **8** to **9** (*21*). Its closest family member described to date, Cg10062 from *Corynebacterium glutamicum*, is considerably homologous in sequence (34% identical and 53% similar) to *cis*-CaaD, and a pairwise alignment suggests that all key catalytic residues of *cis*-CaaD are conserved in Cg10062 (*22*). As expected, Cg10062 possesses dehalogenase activity, converting both **2** and **3** with a strong preference for **3** (*22*).

However, the enzyme exhibits no significant tautomerase activity using **8**.[2] Hence, a functional link of shared promiscuous activities between *cis*-CaaD and a tautomerase from the same family has not yet been identified.

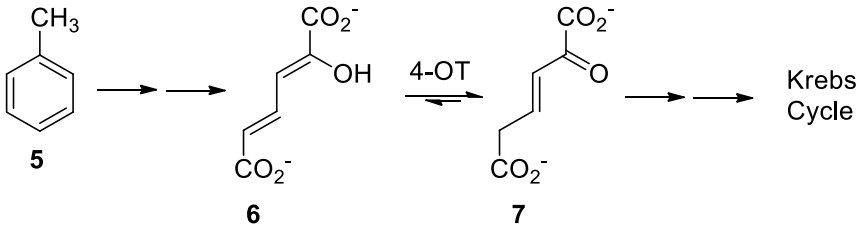

Scheme 2.

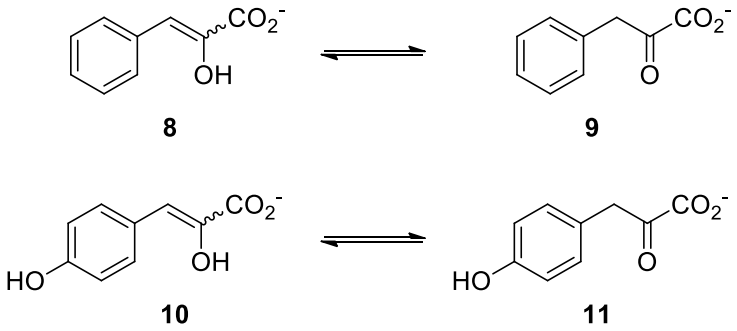

Scheme 3.

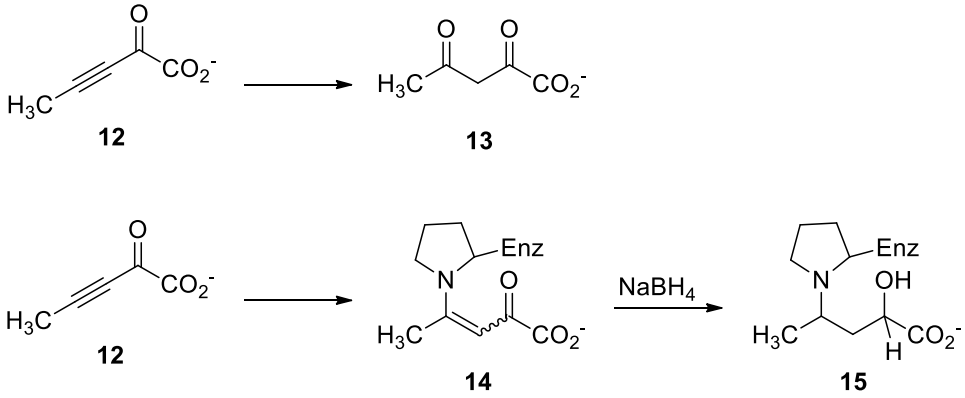

Scheme 4.

As promiscuous activities could provide important clues regarding the progenitor of a newly diverged family member (*7,23,24*), we searched the sequence databases for a homologue of *cis*-CaaD that was tentatively annotated as a putative tautomerase and tested both its phenylenolpyruvate tautomerase (PPT) and *cis*-CaaD activity. Herein, we present the characterization of a *cis*-CaaD homologue (designated MsCCH2) from *Mycobacterium smegmatis* strain MC2 155 that functions as an efficient tautomerase, having a k_{cat}/K_m value of 9.8 x 10^3 M^{-1} s^{-1} for **8**, and has low-level promiscuous *cis*-CaaD and CaaD activity. Hydratase assays and labeling studies using 2-oxo-3-pentynoate (**12**, Scheme 4) indicate that Pro-1 of MsCCH2 has a pK_a value that lies in between that of a typical tautomerase (pK_a of Pro-1 ~6) and that of *cis*-CaaD (pK_a of Pro-1 ~9). These results suggest that MsCCH2 could be characteristic of an evolutionary intermediate along the past route for the divergence of *cis*-CaaD from an unknown homotrimeric tautomerase.

Results

Identification of cis-CaaD Homologues. A sequence similarity search in the NCBI microbial database was performed with the BLASTP program using the *cis*-CaaD amino acid sequence as the query. This search yielded several bacterial proteins that shared significant sequence identity with *cis*-CaaD. The top hits included two sequences from *M. smegmatis* strain MC2 155, designated MsCCH1 and MsCCH2, as well as the previously characterized Cg10062 protein from *C. glutamicum* (Figure 1) (*22*). The mycobacterial protein MsCCH2 is annotated as a putative tautomerase and was selected for further study.

```
cis-CaaD    PVYMVYVSQDRLTPSAKHAVAKAITDAHRGLTGTQHFLAQVNPQEQPAGNVFLGGVQQGG  60
Cg10062     PTYTCWSQRIRISREAKQRIAEAITDAHHELAHAPKYLVQVIPNEVEPDSYFIAAQSASE  60
MsCCH2      PVYTVTMSRGTLNGETKAALAAEITTIHSAVNHVPSTYVNVLPNELAPSNVYTDGKP--A  58
MsCCH1      PLYQIDTVKGRLTPSVKAEIANKVTDIHCQLTGAPDTFVNVVPREYTEGDCFVARKP--E  58
            *                          *

cis-CaaD    DTIFVHGLHREGRSADLKGQLAQRIVDDVSVAAEIDRKHIWVYFGEMPAQQMVEYGRFLP 120
Cg10062     NHIWVQATIRSGRTEKQKEELLLRLTQEIALILGIPNEEVWVYITEIPGSNMTEYGRLLM 120
MsCCH2      HPLIINGWVRTGHSDEQTTALVTQVADAATRITGIPAERVLVIIGNSPARFAIEGGRILP 118
MsCCH1      GRSFLGGQIRHGRSVETRQAMLKALRDMWVQTTGQSEAELIVGISEVDPRMVLEAGFFMP 118
                    *  *                    *           *

cis-CaaD    QPGHEGEWFDNLSSDERAFMETNVDVSRT 149
Cg10062     EPGEEEKWFNSLPEGLRERLTELEGSSE- 148
MsCCH2      DPGQELAWLAATTEQSSGSR--------- 138
MsCCH1      EPGQEKAWFEEHHARLAELGVQAG----- 142
```

Figure 1. Amino acid sequence alignment of *cis*-CaaD from coryneform bacterium strain FG41 (*3*) and three selected *cis*-CaaD homologues. The NCBI reference sequences for the selected proteins are as follows: Cg10062 from *Corynebacterium glutamicum*: NP_599314.1; MsCCH1 from *Mycobacterium smegmatis* strain MC2 155: YP_887666.1; MsCCH2 from *Mycobacterium smegmatis* strain MC2 155: YP_885986.1. Identical residues are shaded in black. The six active site residues of *cis*-CaaD that have been implicated as critical residues for its activity (*3,12*) are indicated by an asterisk.

The mature MsCCH2 protein is predicted to be 138 amino acids in length, assuming excision of the initiating methionine residue. The genomic context of the gene encoding MsCCH2 does not provide any clues about the biological function of this protein in *M. smegmatis*. The sequence of MsCCH2 is 28% identical and 39% similar to that of *cis*-CaaD. Despite the low sequence identity, four of the six active site residues that have been implicated as critical residues for *cis*-CaaD activity (Pro-1, His-28, Arg-70 and Glu-114) are conserved in MsCCH2 (Pro-1, His-28, Arg-68 and Glu-112) (Figure 1) (*3,12*). The other two residues, Arg-73 and Tyr-103, are not conserved and replaced by His-71 and Ile-101 in MsCCH2. To obtain insight into the functional properties of this *cis*-CaaD homologue, MsCCH2 was overproduced, purified and subjected to kinetic and mechanistic characterization (as decribed below).

Expression and Purification of MsCCH2. The gene coding for MsCCH2 was amplified from genomic DNA of *M. smegmatis* strain MC2 155 and cloned into the expression vector pET20b(+), resulting in the construct pMsCCH2. The MsCCH2 encoding gene in pMsCCH2 is under transcriptional control of the T7 promoter, and the enzyme was produced constitutively in *E. coli* BL21(DE3) as a C-terminal hexahistidine fusion protein. The recombinant enzyme was purified by a one-step Ni-Sepharose chromatography protocol, which typically provides ~15 mg of homogeneous enzyme per liter of culture. The purified MsCCH2 was analyzed by electrospray ionization mass spectrometry (ESI-MS) and gel filtration chromatography. Analysis of MsCCH2 by ESI-MS showed one major peak corresponding to a mass of 16093 ± 1 Da. A comparison of this value to the calculated subunit mass (16223 Da) indicates that the initiating methionine is removed during posttranslational processing, which results in a protein with an N-terminal proline. The native molecular mass of MsCCH2 was estimated by gel filtration chromatography to be ~48 kDa, which suggests that the native enzyme is a homotrimeric protein.

Tautomerase Activity of MsCCH2. It has previously been determined that *cis*-CaaD exhibits promiscuous low-level tautomerase activity, converting phenylenolpyruvate (**8**) to phenylpyruvate (**9**) (Scheme 3) (*21*), which may be a vestige of the function of its progenitor. This observation prompted us to examine whether MsCCH2 catalyzes the tautomerization of **8**. The results show that MsCCH2 converts **8** to **9** and that the activity (in terms of k_{cat}) is 170-fold higher than that observed for *cis*-CaaD (Table 1). A comparison of the kinetic parameters further shows that the K_m value for MsCCH2 is significantly higher (32-fold) than that measured for *cis*-CaaD. Together, this results in a 5.4-fold higher k_{cat}/K_m. Additionally, MsCCH2 also catalyzes the conversion of *p*-hydroxyphenylenolpyruvate (**10**) to *p*-hydroxyphenylpyruvate (**11**) (Scheme 3) with a k_{cat} = 3.2 s^{-1} and a K_m of 0.89 mM, resulting in a k_{cat}/K_m of 3.5 × 10^3 M^{-1} s^{-1} (Table 1). The formation of **11** in the reaction of MsCCH2 with **10** was confirmed by ^{1}H NMR spectroscopy (see Supporting Information).

Table 1. Kinetic Parameters for *cis*-CaaD, MsCCH2, and MsCCH2-P1A using Phenylenolpyruvate (**8**) and (*p*-Hydroxyphenyl)enolpyruvate (**10**).

Enzyme	Substrate	k_{cat} (s^{-1})	K_m (μM)	k_{cat}/K_m (M^{-1} s^{-1})
MsCCH2[a]	**8**	34 ± 4	3500 ± 300	9.8×10^3
MsCCH2[a]	**10**	3.2 ± 0.3	890 ± 90	3.5×10^3
P1A-MsCCH2[a]	**8**	0.8 ± 0.02	250 ± 30	3.3×10^3
P1A-MsCCH2[a]	**10**	0.2 ± 0.02	790 ± 150	2.5×10^2
cis-CaaD[b]	**8**	0.2 ± 0.03	110 ± 30	1.8×10^3

[a] These steady-state kinetic parameters were measured in 10 mM Na_2HPO_4 buffer (pH 7.3) at 22 °C. [b] These kinetic data were obtained from Poelarends *et al*. (*21*). Errors are standard deviations.

Dehalogenase Activity of MsCCH2. Having established that MsCCH2 exhibits high-level tautomerase activity, we next investigated whether the enzyme exhibits promiscuous dehalogenase activity. Accordingly, MsCCH2 was incubated with *cis*-3-chloroacrylic acid (**3**) and *trans*-3-chloroacrylic acid (**2**) (Scheme 1), and the reactions were monitored by ^{1}H NMR spectroscopy. After incubation of **3** with MsCCH2 in 100 mM phosphate buffer (pH 9.2) for 14 days at 22 °C, the intensity of the two signals corresponding to **3** (6.25 and 6.17 ppm) decreased and four new signals appeared. Two signals (9.53 and 2.10 ppm) correspond to acetaldehyde, whereas the other two signals (5.11 and 1.18 ppm) correspond to its hydrate. Integration of the signals indicates that ~10% of **3** has been converted to acetaldehyde (and its hydrate). In contrast to *cis*-CaaD, MsCCH2 also processes **2**: ~13% of **2** has been converted to acetaldehyde (and its hydrate) after 14 days at 22 °C.

The MsCCH2-catalyzed conversions of **2** and **3** were also followed in 100 mM phosphate buffer at pH 6.5. Integration of the signals indicates that ~6% of **2** and ~3% of **3** has been converted to acetaldehyde (and its hydrate) after 2 weeks at 22 °C. No product formation was detected for control reactions without enzyme (**2** or **3** incubated in 100 mM phosphate buffer, either pH 6.5 or pH 9.2, for 14 days at 22 °C), ruling out a nonenzymatic dehalogenation.

A previously described colorimetric assay, which monitors halide release, was used to measure kinetic parameters (Table 2) (*1,29*). MsCCH2 catalyzes the dehalogenation of **2** with a k_{cat} = 4×10^{-4} s^{-1} and a K_m of 96 mM, resulting in a k_{cat}/K_m of ~4×10^{-3} M^{-1} s^{-1}. Saturation with **3** was not achieved for MsCCH2 and therefore only the k_{cat}/K_m value was determined. A comparison of this value to that measured for the dehalogenation of **2** shows that MsCCH2 is ~2.5-fold more efficient in catalyzing the dehalogenation of **2** than **3**. In comparison to the *cis*-CaaD-catalyzed dehalogenation of **3**, MsCCH2 shows a 7.5×10^6-fold lower k_{cat}/K_m. Hence, MsCCH2 exhibits low-level dehalogenase activity, accepting both isomers of 3-chloroacrylate as substrates with a slight preference for the *trans*-isomer.

Reaction of MsCCH2 with 2-Oxo-3-Pentynoate. Previous work has shown that the tautomerase 4-OT is irreversibly inactivated by 2-oxo-3-pentynoate (**12**) due to the covalent modification of Pro-1 (*30*), whereas the dehalogenases CaaD and *cis*-CaaD convert **12** to acetopyruvate (**13**) (Scheme 4) (*2,3*). These dissimilar reactions reflect differences in the ionization state and reactivity of Pro-1 in the tautomerase versus dehalogenase active sites. In order to probe the active site of MsCCH2, the reaction of this enzyme with **12** was examined and compared to the well-characterized 4-OT and CaaD reactions with **12**.

Table 2. Kinetic Parameters for *cis*-CaaD, Cg10062, and MsCCH2 Using *cis*-3-chloroacrylate (**3**) and *trans*-3-chloroacrylate (**2**).

Enzyme	Substrate	k_{cat} (s^{-1})	K_m (mM)	k_{cat}/K_m (M^{-1} s^{-1})
MsCCH2[a]	**3**	ND[b]	ND	1.6×10^{-3}
MsCCH2[a]	**2**	$(4.0 \pm 0.1) \times 10^{-4}$	96 ± 6	4.0×10^{-3}
Cg10062[c]	**3**	1.6 ± 0.3	156 ± 42	10
Cg10062[c]	**2**	$(2.0 \pm 1) \times 10^{-3}$	54 ± 40	4.0×10^{-2}
cis-CaaD[c]	**3**	4.6 ± 0.3	0.152 ± 0.02	3.0×10^{4}

[a] The steady-state kinetic parameters were measured in 50 mM Tris-SO_4 buffer (pH 8.0) at 22 °C. [b] Not determined. [c] These kinetic data were obtained from Poelarends *et al.* (*22*). Errors are standard deviations.

As expected, incubation of **12** with CaaD (at pH 7.3) resulted in a decrease in the absorbance at 234 nm, corresponding to **12**, accompanied by the appearance of one new absorbance peak at 294 nm, which corresponds to **13** (Figure 2A) (*2*). Incubation of **12** with 4-OT (at pH 7.3) resulted in the rapid inactivation of 4-OT and the appearance of one new absorbance peak at 340 nm, which likely corresponds to the enamine species **14** (Scheme 4) (Figure 2B) (*30*). Surprisingly, the conversion of **12** by MsCCH2 (at pH 7.3) resulted in the appearance of two new absorbance peaks, one at 294 nm and the other at 324 nm (Figure 2C). From comparison to the product absorbance peaks formed in the reactions of CaaD and 4-OT with **12**, it can be inferred that the peak observed at 294 nm corresponds to acetopyruvate (**13**), whereas the peak observed at 324 nm likely corresponds to an enamine species (**14**), which could result from the reaction between **12** and Pro-1 of MsCCH2. Importantly, the formation of **13** and covalently modified MsCCH2 (presumably **14**) in the reaction of **12** with MsCCH2 was confirmed by ESI-MS and MS/MS analyses (see Supporting Information).

Identification of the Modified Active Site Residue by Mass Spectrometry. In order to identify the site of modification, MsCCH2 was treated with **12** at pH 7.3, reduced with $NaBH_4$,[3] and analyzed by ESI-MS. The reconstruct of the ESI mass spectrum revealed two major peaks, one corresponding to the mass of unmodified MsCCH2 (16094 Da) and the other to the mass expected for the enzyme modified by a single molecule of **12** and reduced by $NaBH_4$ (16209 Da). This MsCCH2 sample was then digested with

endoproteinase Glu-C (*31*), and the resulting peptide mixture was analyzed by MALDI-TOF-MS. A comparison of the peaks of the modified MsCCH2 component to those of the unmodified MsCCH2 component in the peptide mixture revealed a single modification by a species having a mass of 116 Da on the fragments Pro-1 to Glu-15 and Pro-1 to Glu-23 (Table 3). Analysis of the remaining peaks showed no modification of other fragments. These data indicate that a single site on the enzyme has been modified and that the site of modification is localized within the amino-terminal fragment Pro-1 to Glu-15.

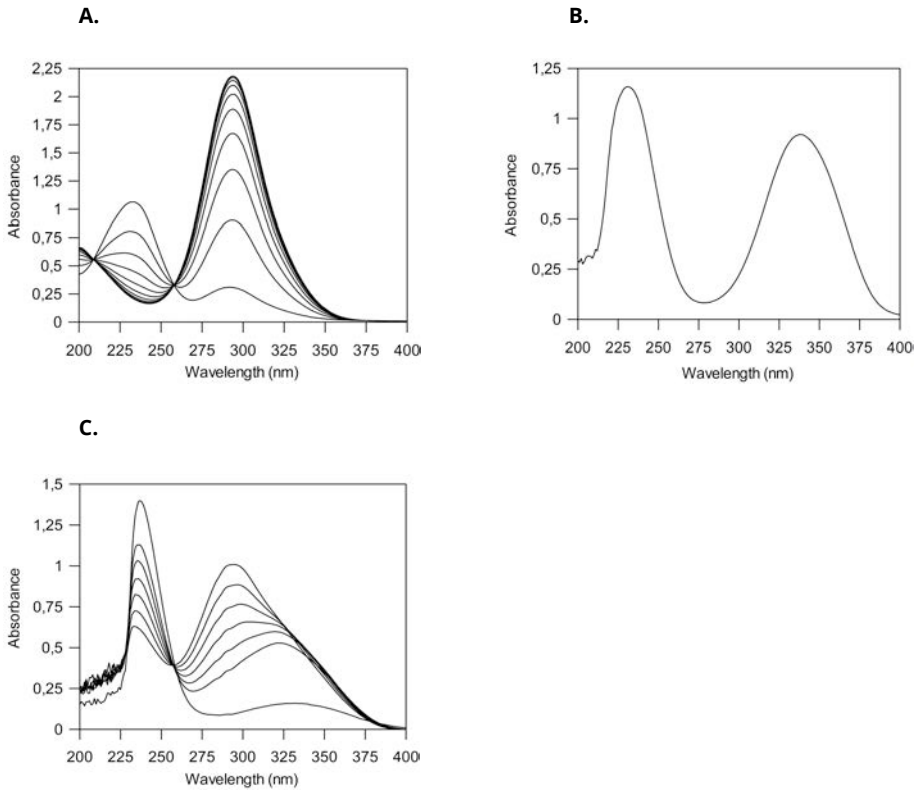

Figure 2. UV spectra monitoring the dissimilar reactions of CaaD, 4-OT and MsCCH2 with 2-oxo-3-pentynoate (**12**, 400 μM) in 10 mM phosphate buffer at pH 7.3. (A) UV spectra monitoring the CaaD-catalyzed conversion of **12** (λ_{max} = 234 nm) to acetopyruvate (**13**, λ_{max} = 294 nm) (*2*). Spectra were recorded every 2 minutes. (B) UV spectrum of 4-OT inactivated by **12**. The absorbance at 234 nm corresponds to unreacted **12**, while the absorbance peak at 340 nm likely corresponds to enamine **14** (Scheme 4), which results from the reaction between **12** and Pro-1 of 4-OT (*30*). (C) UV spectra monitoring the MsCCH2-catalyzed conversion of **12** (λ_{max} = 234 nm). The product peak at 294 nm corresponds to **13**, whereas the peak observed at 324 nm likely corresponds to enamine **14**, which results from the reaction between **12** and Pro-1 of MsCCH2. Spectra were recorded every 40 minutes.

To determine the actual site of the single modification, the unmodified and modified Pro-1 to Glu-15 and Pro-1 to Glu-23 peptides were subjected to MALDI-TOF/TOF-MS analysis. Because the two Pro-1 to Glu-23 peptides gave a more complete fragmentation pattern than the two Pro-1 to Glu-15 peptides, the masses of the fragment ions observed in the TOF/TOF spectra of the modified and unmodified Pro-1 to Glu-23 peptides were further analyzed. The spectrum of the precursor ion corresponding to the unmodified Pro-1 to Glu-23 peptide displayed characteristic b-ions resulting from the peptide fragments PVYTVTMSRGTLN and PV. MALDI-TOF/TOF-MS analysis of the precursor ion corresponding to the modified Pro-1 to Glu-23 peptide revealed an increase in mass of 116 Da for these b-ions (Table 3). Because one of these fragment ions is generated by the dipeptide Pro-1 to Val-2, we conclude that the active site Pro-1 residue is the sole site of modification by **12**.

Table 3. Identification of Pro-1 as the sole site of labeling by **12** using Glu-C digestion and MALDI-TOF-MS and MALDI-TOF/TOF-MS analyses.

Peptide fragment	Calculated mass (Da) [a]	Observed mass (Da)
PVYTVTMSRGTLNGE	1624.8	1625.5
$C_5H_8O_3$-PVYTVTMSRGTLNGE	1740.8	1741.6
PVYTVTMSRGTLNGETKAALAAE	2380.2	2381.8 [b]
PVYTVTMSRGTLN	1420.7	1421.9 [c]
PV	197.1	197.1 [c]
$C_5H_8O_3$-PVYTVTMSRGTLNGETKAALAAE	2496.2	2497.8 [b]
$C_5H_8O_3$-PVYTVTMSRGTLN	1536.7	1537.9 [c]
$C_5H_8O_3$-PV	313.1	313.2 [c]

[a] These values are calculated using the average molecular mass. [b] This value corresponds to the total mass of the parent ion. [c] The reported mass corresponds to the b-ion.

Effect of pH on Product Formation in Incubations of MsCCH2 with 2-Oxo-3-Pentynoate. To probe the ionization state of Pro-1, the reaction of MsCCH2 with **12** was examined at three different pH values (Figures 3 and 4). Incubation of MsCCH2 with **12** at pH 6.5 resulted in the formation of **13**, but no absorbance peak at 324 nm (indicative of covalently modified MsCCH2; that is, the presumed enamine species **14**) was observed (Figure 3A). Indeed, analysis of this incubation mixture by ESI-MS showed one major peak corresponding to the mass (16093) of unmodified MsCCH2 (Figure 4A). These observations suggest that MsCCH2 exhibits hydratase activity at pH 6.5, converting **12** to **13**, which implies that Pro-1 is cationic at pH 6.5 and not functioning as nucleophile. However, incubation of **12** with MsCCH2 at pH 8.5 did not result in formation of **13**, but only resulted in the formation of covalently modified MsCCH2, as indicated by the absorbance peak at 324 nm (Figure 3C). As expected, analysis of this incubation mixture by ESI-MS showed one major peak corresponding to the mass (16206) of modified

MsCCH2 (Figure 4C). This suggests that at pH 8.5, Pro-1 has the correct protonation state to be able to act as a nucleophile and attacks **12** to form a covalently modified enzyme (**14**). Consistent with the preceding experiment at pH 7.3, incubation of **12** with MsCCH2 at pH 7.5 resulted in the formation of both **13** and covalently modified enzyme (Figures 3B and 4B). Assuming a pK_a of Pro-1 of about 7.5, ~50% of the enzyme would be in the correct protonation state to react with **12** to give **13**, and ~50% of the enzyme would be in the correct protonation state to attack **12** to give **14**.

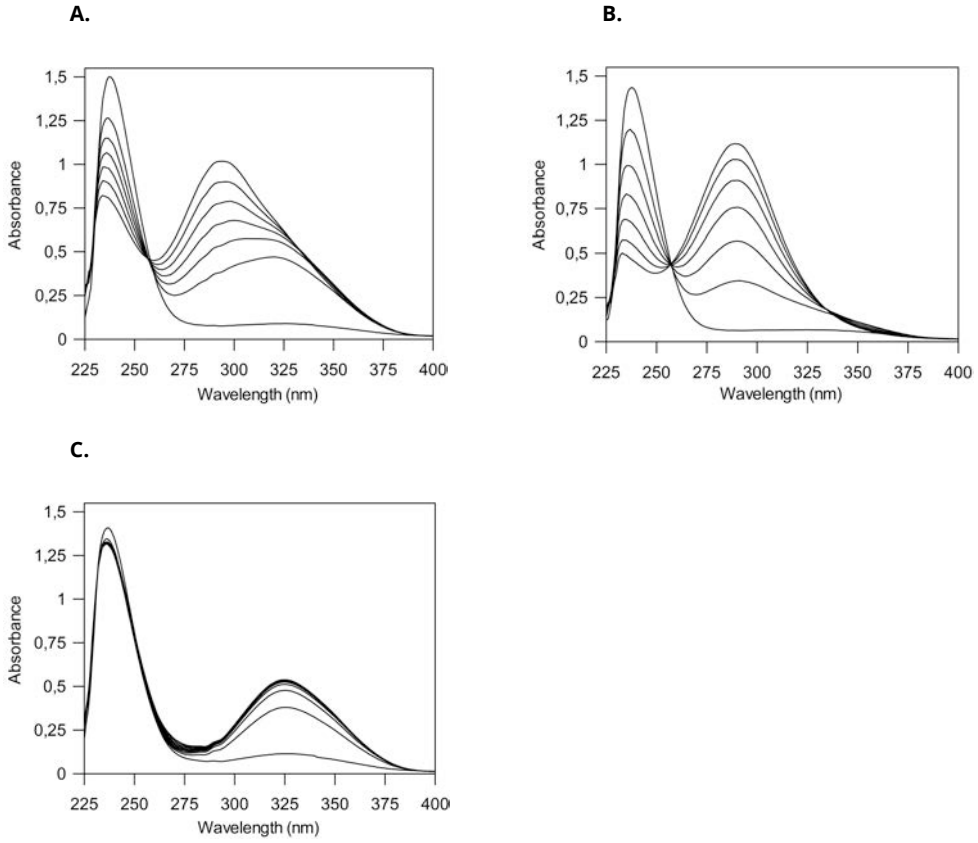

Figure 3. UV spectra monitoring the reaction of MsCCH2 with 2-oxo-3-pentynoate (**12**, 400 μM) in 10 mM phosphate buffer at three different pH values. (A) Spectra monitoring the reaction at pH 6.5. Spectra were recorded every 40 minutes. (B) Spectra monitoring the reaction at pH 7.5. Spectra were recorded every 40 minutes. (C) Spectra monitoring the reaction at pH 8.5. Spectra were recorded every 5 minutes. The decrease in absorbance at 234 nm corresponds to the loss of **12**, whereas the increases in absorbance at 294 nm and 324 nm correspond to the formation of **13** and **14**, respectively.

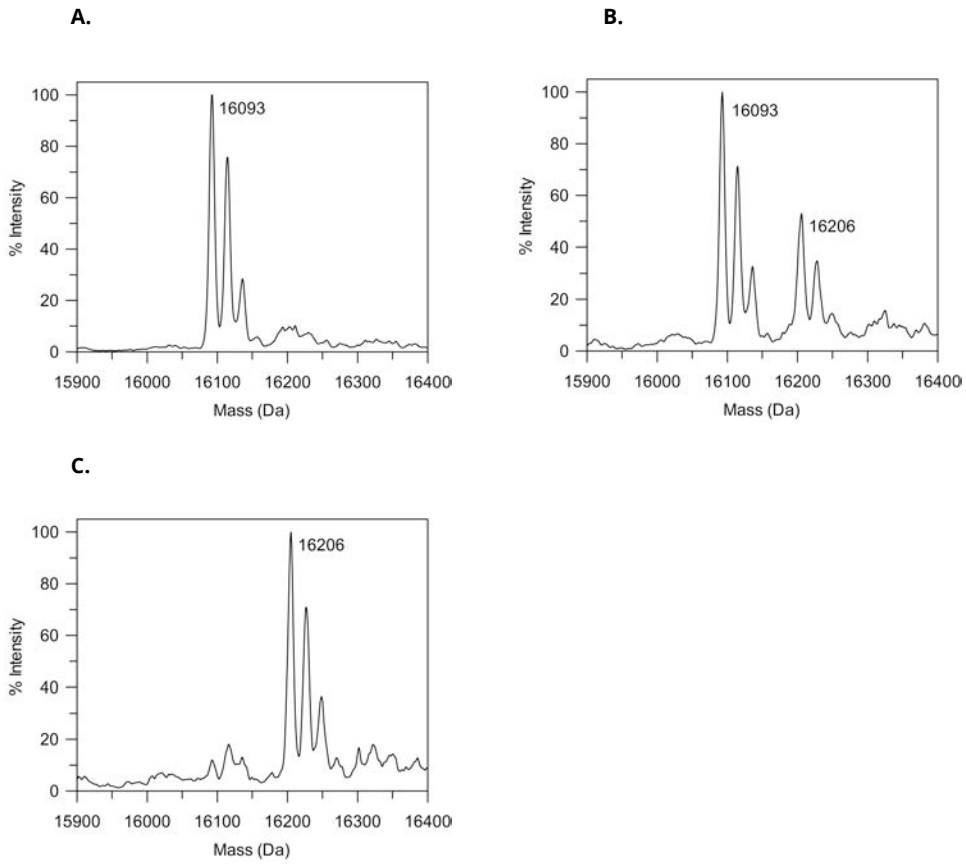

Figure 4. ESI-MS analysis of the MsCCH2 protein in the three incubation mixtures described in Figure 3. (A) ESI-MS analysis of MsCCH2 after incubation with **12** at pH 6.5; see Figure 3A. (B) ESI-MS analysis of MsCCH2 after incubation with **12** at pH 7.5; see Figure 3B. (C) ESI-MS analysis of MsCCH2 after incubation with **12** at pH 8.5; see Figure 3C. The major peaks in the spectra correspond to either unmodified MsCCH2 (16093 Da) or MsCCH2 modified by a single molecule of **12** (16206 Da). The additional minor peaks at the right of each major peak result from (one or two) sodium adducts.

Kinetic Properties of the P1A Mutant of MsCCH2. The results above show that incubation of MsCCH2 with **12** (at pH 8.5) leads to the modification of Pro-1 and the concomitant loss of hydratase activity. To further assess the importance of Pro-1 for the activities of MsCCH2, the P1A mutant was constructed, overproduced in *E. coli* BL21(DE3) as a C-terminal hexahistidine fusion protein, and purified to homogeneity using the metal affinity chromatography protocol developed for wild-type MsCCH2. ESI-MS analysis revealed a mass of 16067 Da (calc. 16066 Da for the enzyme without the initiating methionine) for the P1A mutant, indicating that the initiating methionine is removed during posttranslational processing. The kinetic properties of the P1A mutant

were analyzed using **2**, **3**, **8**, **10**, and **12** as substrates, and compared to those measured for the wild-type enzyme.

For **8**, the P1A mutant showed a 41-fold decrease in k_{cat} and a 14-fold decrease in K_m, resulting in a ~3-fold decrease in k_{cat}/K_m (Table 1). For **10**, the P1A mutant showed a 16-fold decrease in k_{cat}, whereas the K_m was not significantly affected. Hence, this resulted in a 16-fold decrease in k_{cat}/K_m. The P1A mutant had no detectable dehalogenase activity towards **2** and **3** using the colorimetric assay, and no detectable activity towards **12** (at pH 7.3) using the UV spectroscopic assay (i.e., the reaction mixture showed no product absorbance peaks). The CaaD and *cis*-CaaD activities of the P1A mutant were also assessed by ^{1}H NMR spectroscopy after a lengthy incubation period (14 days at 22 °C) in 100 mM phosphate buffer (pH 9.2). However, the reaction mixtures showed no product. These findings are not surprising in view of the low-level dehalogenase activities of the wild-type enzyme. Taken together, the results suggest that Pro-1 is critical for the tautomerase, dehalogenase, and hydratase activities of MsCCH2.

Discussion

The mycobacterial enzyme (MsCCH2) characterized in this study proficiently tautomerizes phenylenolpyruvate (**8**) to phenylpyruvate (**9**) and *p*-hydroxyphenylenolpyruvate (**10**) to *p*-hydroxyphenylpyruvate (**11**) (Scheme 3). MsCCH2 catalyzes the conversion of **8** to **9** with a k_{cat}/K_m of 9.8 x 10^3 M^{-1} s^{-1}, which is somewhat lower (~40-fold) than the values measured for the same conversion catalyzed by the tautomerases 4-OT (k_{cat}/K_m = 3.7 x 10^5 M^{-1} s^{-1}) (*32*) and YwhB (k_{cat}/K_m = 4.2 x 10^5 M^{-1} s^{-1}) (*19*). The lower catalytic efficiency of the MsCCH2-catalyzed reaction results mainly from a higher K_m value, which suggests suboptimal binding of **8** in the active site of MsCCH2. A comparison of the kinetic parameters for the MsCCH2 (k_{cat} = 3.2 ± 0.3 s^{-1}, K_m = 890 ± 90 μM) and YwhB (k_{cat} = 4.1 ± 0.4 s^{-1}, K_m = 160 ± 22 μM) (*19*) catalyzed conversion of **10** to **11** shows similar catalytic efficiencies for both enzymes. It is important to emphasize that we have also tested compound **6**, the native substrate of 4-OT (Scheme 2) (*18,19*), as potential substrate for MsCCH2, but no detectable 1,5-keto-enol tautomerase activity was observed. These results indicate that MsCCH2 functions as an effective 1,3-keto-enol tautomerase, converting **8** to **9** and **10** to **11**, given that the physiological substrate for this tautomerase has yet to be identified.

Similarities in sequence and quaternary structure firmly link MsCCH2 to the *cis*-CaaD family, which is one of the five known families in the tautomerase superfamily (*3,12*). With the previously studied family members being *cis*-CaaD (*3*) and Cg10062 (*22*), MsCCH2 is the first known family member that exhibits a pronounced tautomerase activity. All known tautomerase superfamily members are characterized by a catalytic amino-terminal proline (*6,7*). The importance of the conserved Pro-1 in MsCCH2 for its tautomerase activity was demonstrated by mutating this residue to an alanine. For both substrates (**8** and **10**), the major effect of this mutation is observed in k_{cat} (Table 1). Hence, the function of Pro-1 is predominantly catalytic. In the well-studied tautomerases 4-OT and YwhB, the catalytic Pro-1 functions as the general base and is responsible for proton transfer (*19,33-35*). It is therefore reasonable to suggest that

Pro-1 in MsCCH2 also functions as the general base and may abstract the C-2 enol proton (of **8** or **10**) for delivery to the C-3 position (yielding **9** or **11**).

MsCCH2 also exhibits dehalogenase activity using *trans*-3-chloroacrylate (**2**) and *cis*-3-chloroacrylate (**3**) as substrates (Scheme 1), but this activity is much lower (10^6-fold) compared to its tautomerase activity (as assessed by k_{cat}/K_m values). Hence, the tautomerase activity is the primary activity of MsCCH2. A comparison of the kinetic parameters for the conversion of **3** to **4** shows that the catalytic efficiency (k_{cat}/K_m) of MsCCH2 is 10^4- and 10^7-fold lower than that of Cg10062 and *cis*-CaaD (Table 2) (*22*). Unlike *cis*-CaaD, MsCCH2 also catalyzes the conversion of **2** to **4** but with a catalytic efficiency that is 10-fold lower than that measured for Cg10062 (Table 2). Replacement of Pro-1 by an alanine completely abolished the dehalogenase activity of MsCCH2, indicating that dehalogenation, like tautomerization, is an active site process that involves Pro-1.

Although MsCCH2 has a low-level dehalogenase activity, the rates of dehalogenation are still significant in comparison with the reported nonenzymatic rate of ~2.2 x 10^{-12} s^{-1} at 25 °C and pH 7 (*36*). Using this value for the spontaneous, uncatalyzed dehalogenation of **2** and the k_{cat} value for the MsCCH2-catalyzed dehalogenation of **2** (Table 2), it can be estimated that MsCCH2 affords a ~2 x 10^8-fold rate enhancement. Although the individual k_{cat} value for the MsCCH2-catalyzed dehalogenation of **3** could not be determined, a similar 10^8-fold rate enhancement can be assumed. For comparison, *cis*-CaaD, which is thought to have evolved for the purpose of degrading **3** (*3,6*), affords a ~2 x 10^{12}-fold rate enhancement for the conversion of **3** to **4**.

On the basis of experimental studies (*3,11-13*), a mechanism for the *cis*-CaaD-catalyzed conversion of **3** to **4** was proposed (Scheme 5). The first step in catalysis is the nucleophilic attack of an activated water molecule on C-3 of **3** to form an enediolate intermediate. The enzyme presumably uses the side chains of two residues, Glu-114 and Tyr-103, to activate the nucleophilic water molecule. The side chains of His-28, Arg-70, and Arg-73 interact with the C-1 carboxylate group of **3**. These interactions position and polarize the substrate to facilitate the attack of water and stabilize the resulting enediolate species. Tautomerization of the enediolate intermediate may be assisted by Pro-1, which is thought to place a proton at the C-2 atom, and generates an unstable chlorohydrin intermediate (Scheme 5a). Collapse of the proposed chlorohydrin to afford **4** and HCl could be an enzymatic or a nonenzymatic process. Alternatively, the enediolate species can undergo an elimination reaction to release the chlorine as chloride ion, followed by tautomerization of the enol intermediate and protonation at C-2 by Pro-1, yielding **4** (Scheme 5b).

In the context of this proposed *cis*-CaaD mechanism, the much lower dehalogenase activity of MsCCH2 (compared to *cis*-CaaD) could potentially be explained by active site differences. Sequence comparisons suggested that four of the six active site residues that have been implicated as critical residues for *cis*-CaaD activity (Pro-1, His-28, Arg-70 and Glu-114) are conserved in MsCCH2 (Pro-1, His-28, Arg-68 and Glu-112) (Figure 1) (*3,12*). However, two active site residues, Arg-73 and Tyr-103, are replaced by His-71 and

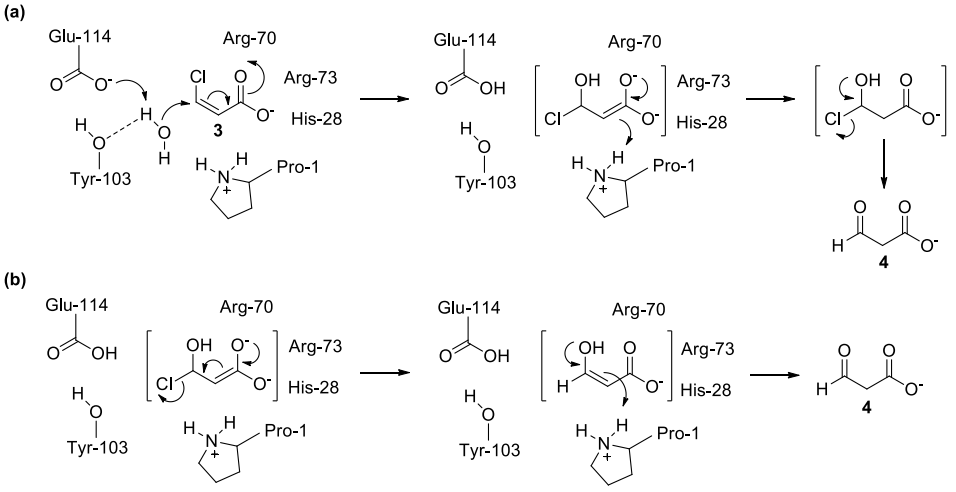

Scheme 5.

Ile-101 in MsCCH2. The replacement of Arg-73 in *cis*-CaaD by His-71 in MsCCH2 may result in less efficient binding and polarization of **3**, thereby affecting water addition. The replacement of Tyr-103 in *cis*-CaaD by Ile-101 in MsCCH2 may even be more significant because it eliminates one of the presumed water-activating residues. These active site differences may reflect the different reaction specificities of MsCCH2 and *cis*-CaaD, and suggest that MsCCH2 could be only a few mutations away from being a highly specific and efficient *cis*-CaaD. Hence, mutation of His-71 to an arginine accompanied by the replacement of Ile-101 with a tyrosine might increase the dehalogenase activity and decrease the tautomerase activity of MsCCH2. The consequences of these mutations are currently being examined.

Another potential explanation for the lower dehalogenase activity and increased tautomerase activity of MsCCH2 could be a lowered pK_a of its Pro-1 residue when compared to the pK_a of Pro-1 (~9.3) in *cis*-CaaD (*11*).[4] Support for this view comes from studies with 2-oxo-3-pentynoate (**12**, Scheme 4). Previous work has shown that the reactions of 4-OT and CaaD, the best characterized members of the 4-OT family in the tautomerase superfamily, with **12** reflect both the ionization state of Pro-1 (neutral versus cationic) and the environment of the active site (*2,30*). Whereas 4-OT is irreversibly inactivated by **12** due to the covalent modification of Pro-1, CaaD converts **12** to acetopyruvate (**13**) (Scheme 4). These dissimilar reactions reflect differences between the two active sites. Pro-1 of 4-OT has a pK_a of ~6.4, enabling it to function as a general base catalyst in its physiological tautomerase activity (conversion of **6** to **7**, Scheme 2) (*33,34*). Hence, at neutral pH, Pro-1 functions as a nucleophile and attacks C-4 of **12** in a Michael-type reaction, presumably yielding **14** (Scheme 4) (*30*). In contrast, the pK_a of Pro-1 in CaaD is ~9.2, enabling it to function as a general acid catalyst in its physiological dehalogenase activity (conversion of **2** to **4**, Scheme 1) (*10*). Thus, a Michael-type reaction between the amino group of proline and **12** is not favored, and in

the active site of CaaD, which has evolved to carry out water addition, **12** is processed to **13** (*2*). Like CaaD, *cis*-CaaD and Cg10062 process **12** to **13**, instead of being inactivated by **12**, which implies that their Pro-1 residues have a pK_a comparable to that determined for Pro-1 of CaaD (*3,22*).

In view of these observations, the reaction of MsCCH2 with **12** was examined at different pH values. At pH 8.5, MsCCH2 is inactivated by **12** due to the covalent modification of Pro-1. This suggests that Pro-1 is neutral at pH 8.5 and functions as a nucleophile, attacking C-4 of **12** in a Michael-type reaction. The identification of **15** by mass spectrometry experiments, coupled with the observed λ_{max} of 324 nm for the reaction product, strongly suggests that the reaction results in the formation of **14**. Indeed, reduction with $NaBH_4$ results in the complete loss of the absorbance at 324 nm, consistent with the rearrangement of **14** into the corresponding imine, which is reduced by $NaBH_4$ to give **15**. At pH 6.5, however, MsCCH2 exhibits hydratase activity and converts **12** to **13**. This implies that Pro-1 is cationic at pH 6.5 and not functioning as a nucleophile. At pH 7.3-7.5, MsCCH2 converts **12** to both **13** and **14**, indicating that the hydratase and inactivation reactions occur simultaneously. These observations, coupled with the results of control reactions using **12** and 4-OT or CaaD at pH 7.3, suggest that Pro-1 of MsCCH2 has a pK_a value that lies in between that of a typical tautomerase like 4-OT (pK_a of Pro-1 ~6.4) and that of the dehalogenases CaaD and *cis*-CaaD (pK_a of Pro-1 ~9.2). This makes MsCCH2 the first known tautomerase superfamily member with such an intermediate pK_a value for its catalytic Pro-1 residue. This intermediate pK_a value, estimated to be ~7.5, may enable Pro-1 to serve (at cellular pH) as a general base catalyst in its primary tautomerase activity and as a general acid catalyst in its promiscuous dehalogenase activity.

Given that Pro-1 in CaaD and *cis*-CaaD has a pK_a of ~9.2 (*10,11*), enabling it to function as a general acid catalyst in the physiological dehalogenase activity, an interesting route for the laboratory evolution of MsCCH2 into a more efficient dehalogenase can be proposed. The introduction of one or more hydrophilic residues could make the active site of MsCCH2 less hydrophobic, thereby making the active site more amenable for water addition as well as raising the pK_a of Pro-1. This would increase the concentration of enzyme with Pro-1 in the correct protonation state to function as a general acid catalyst. The appropriate experiments to investigate this intriguing possibility are underway.

In conclusion, the identification of MsCCH2 as tautomerase with promiscuous dehalogenase and hydratase activities now establishes a functional link between the recently diverged *cis*-CaaD and a tautomerase of the same family. Hence, the major phenylpyruvate tautomerase activity of MsCCH2 comprises the promiscuous activity of *cis*-CaaD, and the primary dehalogenase activity of *cis*-CaaD comprises the promiscuous activity of MsCCH2. In addition, both enzymes possess significant hydratase activity. A reasonable route for the divergence of *cis*-CaaD from an unknown tautomerase is presented in Figure 5. The ancestral tautomerase may have been a specialist tautomerase with a low pK_a value for its catalytic Pro-1 residue. Mutations in the

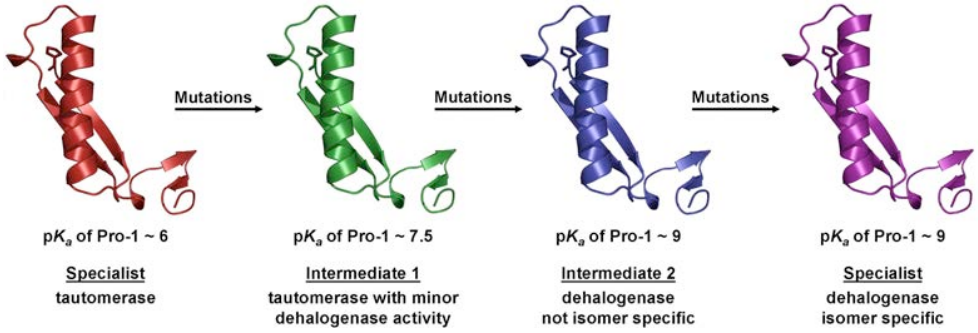

Figure 5. Proposed evolutionary pathway for the divergence of an ancestral tautomerase, which may have been a specialist, to *cis*-CaaD, a specialist dehalogenase that is selective for the *cis*-isomer of 3-chloroacrylate (*3*). The family members MsCCH2 (this study) and Cg10062 (*22*) could be characteristic of evolutionary intermediates 1 and 2, respectively. In the course of divergence, the pK_a of the essential Pro-1 residue likely increased from ~6 (in the ancestral tautomerase) to ~7.5 (in the generalist intermediate 1) to ~9 (in the specialist dehalogenase), allowing this residue to efficiently serve as a general acid in the newly evolved dehalogenase activity. For clarity, and because the three-dimensional structures of MsCCH2 and Cg10062 are not reported yet, the β-α-β building block carrying the N-terminal proline is shown.

specialist may have raised the pK_a of its Pro-1 residue to about 7.5. This may have introduced a low-level promiscuous dehalogenase activity in the enzyme, without significantly decreasing the original tautomerase activity. This thus yielded, in effect, a generalist intermediate (intermediate 1 in Figure 5) exhibiting both tautomerase and dehalogenase activity. MsCCH2 could be characteristic of this generalist intermediate, and may therefore resemble the progenitor of *cis*-CaaD, using its promiscuous dehalogenase activity as an essential starting point. Further mutation and selection for an increase of the promiscuous dehalogenase activity may have resulted in intermediate 2, and finally in the specialist dehalogenase, *cis*-CaaD. Cg10062, which has pronounced dehalogenase activity, but lacks isomer specificity (*22*), could be characteristic of intermediate 2. In the course of divergence, the pK_a of the essential Pro-1 residue likely increased from ~6 (in the ancestral tautomerase) to ~7.5 (in the generalist intermediate 1) to ~9 (in intermediate 2 and the specialist dehalogenase), allowing this residue to efficiently serve as a general acid in the newly evolved dehalogenase activity. Although this route is highly speculative, laboratory evolution of the promiscuous dehalogenase activity of MsCCH2 could provide important insight into pathways that could lead to the rapid divergent evolution of an efficient *cis*-CaaD enzyme.

Acknowledgements
We thank Professor William R. Jacobs, Jr. (Howard Hughes Medical Institute, Chevy Chase, MD) for the kind gift of genomic DNA of *Mycobacterium smegmatis* strain MC2 155 and Professor Christian P. Whitman (University of Texas at Austin, TX) for the kind gift of 2-oxo-3-pentynoate. We thank Annie van Dam and Margot Jeronimus-Stratingh (University of Groningen) for their expert assistance in acquiring the MS spectra.

Materials and methods
Materials. The sources of the chemicals, biochemicals, components of buffers and media, PCR purification, gel extraction, and Miniprep kits, Ni-NTA sepharose, pre-packed PD-10 Sephadex G-25 columns, and the oligonucleotides, enzymes and reagents used in the molecular biology procedures are reported elsewhere (*25*). Phenylpyruvate, (*p*-hydroxyphenyl)-pyruvate, *trans*-3-chloroacrylic acid, and *cis*-3-chloroacrylic acid were purchased from Sigma-Aldrich Chemical Co. (St. Louis, MO). 2-Oxo-3-pentynoate was a kind gift of Professor C.P. Whitman (University of Texas at Austin, TX).

General Methods. BLASTP searches of the National Center for Biotechnology Information (NCBI) databases were performed using the *cis*-CaaD amino acid sequence (GenBank: AAR00932.1) as the query sequence. Amino acid sequences were aligned using a version of the CLUSTALW multiple-sequence alignment routines available in the computational tools at the EMBL-EBI Website. Techniques for restriction enzyme digestions, ligation, transformation, and other standard molecular biology manipulations were based on methods described elsewhere (*26*) or as suggested by the manufacturer. The PCR was carried out in a DNA thermal cycler (model GS-1) obtained from Biolegio (Nijmegen, The Netherlands). DNA sequencing was performed by ServiceXS (Leiden, The Netherlands) or Macrogen (Seoul, Korea). Protein was analyzed by sodium dodecyl sulfate-polyacrylamide gel electrophoresis (SDS-PAGE) on gels containing 10% polyacrylamide. The gels were stained with Coomassie brilliant blue. Protein concentrations were determined by the method of Waddell (*27*). Kinetic data were obtained on a V-650 or V-660 spectrophotometer from Jasco (IJsselstein, The Netherlands). The kinetic data were fitted by nonlinear regression data analysis using the Grafit program (Erithacus, Software Ltd., Horley, U.K.) obtained from Sigma Chemical Co. ^{1}H NMR spectra were recorded on a Varian Inova 500 (500 MHz) spectrometer using a pulse sequence for selective presaturation of the water signal. Chemical shifts for protons are reported in parts per million scale (δ scale) downfield from tetramethylsilane and are referenced to protium (H_2O: δ = 4.67). The native molecular mass of purified MsCCH2 was determined by Superdex 75 gel filtration using a fast protein liquid chromatography system according to the instructions provided with the HiLoad 16/60 Superdex 75 prep grade column (Pharmacia). The standard molecular mass markers were albumin (67 kDa), ovalbumin (43 kDa), chymotrypsinogen A (25 kDa) and ribonuclease A (13.7 kDa). ESI-MS and MS/MS spectra were recorded using an LCQ electrospray mass spectrometer (Applied Biosystems, Foster City, CA). MALDI-TOF and TOF/TOF mass spectra were recorded using a 4700 Proteomics Analyzer (Applied

Biosystems). The enzymes CaaD and 4-OT were purified according to a previously published procedure (*28*).

Construction of Expression Vectors for MsCCH2 and the MsCCH2-P1A Mutant, and Expression and Purification of the two His-Tagged Proteins. The experimental procedures used for the construction of expression vectors for MsCCH2 wild-type and the MsCCH2-P1A mutant, and the overproduction and purification of these two proteins are provided in the Supporting Information.

Enzyme Assays. The tautomerization activities of MsCCH2 and the P1A mutant were measured by monitoring the ketonization of **8** to **9** and **10** to **11** in 10 mM Na_2HPO_4 buffer (pH 7.3) at 22 ^{o}C. Stock solutions of **8** and **10** were generated by dissolving the appropriate amount of phenylpyruvic acid or (*p*-hydroxyphenyl)pyruvic acid in absolute ethanol. The crystalline free acid of phenylpyruvic acid or (*p*-hydroxyphenyl)pyruvic acid is exclusively the enol form. The ketonization of **8** to **9** was monitored by following the decrease in absorbance at either 310 nm (ε = 1400 M^{-1} cm^{-1}) or 315 nm (ε = 300 M^{-1} cm^{-1}) using substrate concentrations ranging from 0.05 to 8 mM. The ketonization of **10** to **11** was monitored by following the decrease in absorbance at 325 nm (ε = 1800 M^{-1} cm^{-1}) using substrate concentrations ranging from 0.1 to 1.8 mM. An appropriate quantity of enzyme (from a 5 mg/mL stock solution in 10 mM Na_2HPO_4 buffer, pH 7.3) was diluted into the sodium phosphate buffer (1 mL in a cuvette), and the assay was initiated by the addition of a small aliquot (5-20 μL) of substrate (either **8** or **10**) from a stock solution. At all substrate concentrations, the nonenzymatic rate was subtracted from the enzymatic rate of ketonization.

The dehalogenation activities of MsCCH2 and the P1A mutant were measured by following the dechlorination of **2** and **3** at 22 ^{o}C in 50 mM Tris-SO_4 buffer (pH 8.0) using a colorimetric assay (*1,29*). An appropriate amount of enzyme (1 mg) was incubated with the desired concentration of **2** or **3** in 3 mL of the Tris-SO_4 buffer.

The concentrations of substrate in the assay ranged from 20 to 350 mM. Stock solutions (400 mM) of **2** and **3** were made up in 50 mM Tris-SO_4 buffer. The pH of the stock solution was adjusted to 8.0. Chloride concentrations were measured colorimetrically at different time intervals.

*^{1}H NMR Spectroscopic Analysis of the Reaction of MsCCH2 with **2**, **3** or **10**.* ^{1}H NMR spectra monitoring the MsCCH2-catalyzed conversion of *trans*-3-chloroacrylate (**2**), *cis*-3-chloroacrylate (**3**), or (*p*-hydroxyphenyl)enolpyruvate (**10**) were recorded according to protocols reported elsewhere (*2,3,25*). The modifications to these protocols are provided in the Supporting Information.

*UV Spectroscopic Analysis of the Reactions of CaaD, 4-OT, and MsCCH2 with 2-Oxo-3-Pentynoate (**12**).* UV spectra monitoring the CaaD, 4-OT, and MsCCH2 reactions with **12** were recorded as follows. An appropriate amount of enzyme (45 μg of CaaD, 0.5 mg of 4-OT or 0.5 mg of MsCCH2) was incubated with **12** (400 μM) in 1 mL of 10 mM Na_2HPO_4 buffer at 22 °C, with the final pH of the incubation mixture ranging from 6.5 to 8.5. A fresh stock solution of **12** (40 mM) was made up in 10 mM Na_2HPO_4 buffer, and the pH was adjusted to 7.3. The hydration of **12** (λ_{max} = 234 nm) was monitored by following the formation of **13** at 294 nm (*2*). The covalent modification of 4-OT or MsCCH2 by **12** was

monitored by following the formation of **14** (for 4-OT, λ_{max} = 340 nm; for MsCCH2, λ_{max} = 324 nm).

To determine the mass of (unmodified and modified) MsCCH2 after its incubation with **12** in 10 mM Na_2HPO_4 buffer at pH 6.5, 7.3, 7.5, or 8.5, a sample was withdrawn from the incubation mixture, diluted 10-fold in 5 mM NH_4HCO_3 buffer (pH 7.3), and directly analyzed by ESI-MS.

*Mass Spectral Analysis of the Product of the MsCCH2-Catalyzed Hydration of 2-Oxo-3-Pentynoate (**12**)*. The experimental procedure used for the identification of **13** as the product of the MsCCH2-catalyzed hydration of **12** is provided in the Supporting Information.

Mass Spectral Analysis of Modified MsCCH2 and Peptide Mapping. The MsCCH2 sample was made up as follows. The enzyme (1 mg) was incubated with **12** (400 μM) in 1 mL of 10 mM NaH_2PO_4 buffer (pH 7.3) for 3 h at 22 °C. The formation of the covalent adduct (**14**) was monitored spectrophotometrically at 324 nm. An aliquot of a 500 mM stock solution of $NaBH_4$ in water was added to the sample to give a final $NaBH_4$ concentration of 25 mM, after which the mixture was incubated overnight at 22 °C. This protocol was repeated (3 times) until the absorbance at 324 nm was completely lost. Subsequently, the buffer was exchanged against 5 mM NH_4HCO_3 buffer (pH 7.3) using a pre-packed PD-10 Sephadex G-25 gelfiltration column. An aliquot of this protein sample was directly analyzed by ESI-MS.

For the peptide mapping studies, a quantity (50 μg) of the MsCCH2 sample was vacuum-dried. The protein pellet was dissolved in 10 μL of 10 M guanidine-HCl and incubated for 2 h at 37 ^{o}C. Subsequently, the sample was diluted 10-fold by the addition of 90 μL of 100 mM NH_4HCO_3 buffer (pH 8.0) and incubated for 48 h at 37 ^{o}C with protease Glu-C (0.5 μL from a 10 mg/mL stock solution in water). The sample was analyzed by MALDI-TOF MS without further purification. Selected ions of modified and umodified peptide fragments were subjected to TOF/TOF MS analysis.

Footnotes

[1]Abbreviations: CaaD, *trans*-3-chloroacrylic acid dehalogenase; *cis*-CaaD, *cis*-3-chloroacrylic acid dehalogenase; EBI, European Bioinformatics Institute; EMBL, European Molecular Biology Laboratory; ESI-MS, electrospray ionization mass spectrometry; MALDI-TOF, matrix assisted laser desorption/ionization time-of-flight; MsCCH, *Mycobacterium smegmatis cis*-CaaD homologue; NCBI, National Center for Biotechnology Information; NMR, nuclear magnetic resonance; 4-OT, 4-oxalocrotonate tautomerase; PCR, polymerase chain reaction; PPT, phenyl(enol)pyruvate tautomerase; SDS-PAGE, sodium dodecyl sulfate-polyacrylamide gel electrophoresis.

[2]G. J. Poelarends and C. P. Whitman, unpublished results.

[3]Without this reduction step, the bound species is lost under the conditions of the MALDI-TOF MS experiments. Reduction with $NaBH_4$ results in the complete loss of the

absorbance at 324 nm, consistent with the rearrangement of the presumed enamine species (**14**, Scheme 4) into the corresponding imine, which is reduced by $NaBH_4$.

[4]The pK_a of the catalytic Pro-1 in CaaD has been determined to be 9.2 by direct titration using ^{15}N NMR spectroscopy (*10*). A direct titration of Pro-1 in *cis*-CaaD has not been conducted, but a pH-rate profile of the *cis*-CaaD reaction implicated an acid catalyst with a pK_a of ~9.3 (*11*). It is assumed that this pK_a value corresponds to that of Pro-1 on the basis of the expected mechanistic parallels with CaaD.

References

1 Poelarends, G. J., Saunier, R., and Janssen, D. B. (2001) *trans*-3-Chloroacrylic acid dehalogenase from *Pseudomonas pavonaceae* 170 shares structural and mechanistic similarities with 4-oxalocrotonate tautomerase, *J. Bacteriol. 183*, 4269–4277.

2 Wang, S. C., Person, M. D., Johnson, W. H., Jr., and Whitman, C. P. (2003) Reactions of *trans*-3-chloroacrylic acid dehalogenase with acetylene substrates: Consequences of and evidence for a hydration reaction, *Biochemistry 42*, 8762–8773.

3 Poelarends, G. J., Serrano, H., Person, M. D., Johnson, W. H., Jr., Murzin, A. G., and Whitman, C. P. (2004) Cloning, expression, and characterization of a *cis*-3-chloroacrylic acid dehalogenase: Insights into the mechanistic, structural, and evolutionary relationship between isomer-specific 3-chloroacrylic acid dehalogenases, *Biochemistry 43*, 759–772.

4 van Hylckama Vlieg, J. E. T., and Janssen, D. B. (1992) Bacterial degradation of 3-chloroacrylic acid and the characterization of *cis*- and *trans*-specific dehalogenases, *Biodegradation 2*, 139–150.

5 Poelarends, G. J., Wilkens, M., Larkin, M. J., van Elsas, J. D., and Janssen, D. B. (1998) Degradation of 1,3-dichloropropene by *Pseudomonas cichorii* 170, *Appl. Environ. Microbiol. 64*, 2931–2936.

6 Poelarends, G. J., and Whitman, C. P. (2004) Evolution of enzymatic activity in the tautomerase superfamily: Mechanistic and structural studies of the 1,3-dichloropropene catabolic enzymes, *Bioorg. Chem. 32*, 376–392.

7 Poelarends, G. J., Puthan Veetil, V., and Whitman, C. P. (2008) The chemical versatility of the β-α-β fold: catalytic promiscuity and divergent evolution in the tautomerase superfamily, *Cell. Mol. Life Sci.*, *65*, 3606-3618.

8 Poelarends, G. J., and Whitman, C. P. (2010) Mechanistic and structural studies of microbial dehalogenases: How Nature cleaves a carbon-halogen bond, in *Comprehensive Natural Products II: Chemistry and Biology* (Mander, L.N., and Liu, H.-W., Eds.) volume 8, pp 89-123, Elsevier, Oxford, UK.

9 de Jong, R. M., Brugman, W., Poelarends, G. J., Whitman, C. P., and Dijkstra, B. W. (2004) The X-ray structure of *trans*-3-chloroacrylic acid dehalogenase reveals a novel hydration mechanism in the tautomerase superfamily, *J. Biol. Chem. 279*, 11546–11552.

10 Azurmendi, H. F., Wang, S. C., Massiah, M. A., Poelarends, G. J., Whitman, C. P., and Mildvan, A. S. (2004) The roles of active site residues in the catalytic mechanism of *trans*-3-chloroacrylic acid dehalogenase: A kinetic, NMR, and mutational analysis, *Biochemistry 43*, 4082–4091.

11 Poelarends, G. J., Serrano, H., Johnson, W. H., Jr., and Whitman, C. P. (2004) Stereospecific alkylation of *cis*-chloroacrylic acid dehalogenase by (*R*)-oxirane-2-carboxylate: Analysis and mechanistic implications, *Biochemistry 43*, 7187–7196.

12 de Jong, R. M., Bazzacco, P., Poelarends, G. J., Johnson, W. H., Jr., Kim, Y.-J., Burks, E. A., Serrano, H., Thunnissen, A.-M. W. H., Whitman, C. P., and Dijkstra, B. W. (2007) Crystal structures of native and inactivated *cis*-3-chloroacrylic acid dehalogenase: Structural basis for substrate specificity and inactivation by (*R*)-oxirane-2-carboxylate, *J. Biol. Chem. 282*, 2440–2449.

13 Robertson, B. A., Schroeder, G. K., Jin, Z., Johnson, K. A., and Whitman, C. P. (2009) Pre-steady-state kinetic analysis of *cis*-3-chloroacrylic acid dehalogenase: analysis and implications, *Biochemistry 48*, 11737-11744.

14 Sevastik, R., Whitman, C. P., and Himo, F. (2009) Reaction mechanism of *cis*-3-chloroacrylic acid dehalogenase: a theoretical study, *Biochemistry 48*, 9641-9649.

15 Whitman, C. P. (2002) The 4-oxalocrotonate tautomerase family of enzymes: How nature makes new enzymes using a β-α-β structural motif, *Arch. Biochem. Biophys. 402*, 1–13.

16 Harayama, S., Rekik, M., Ngai, K.-L., and Ornston, L. N. (1989) Physically associated enzymes produce and metabolize 2-hydroxy-2,4-dienoate, a chemically unstable intermediate formed in catechol metabolism via meta cleavage in *Pseudomonas putida*, *J. Bacteriol. 171*, 6251-6258.

17 Chen, L. H., Kenyon, G. L., Curtin, F., Harayama, S., Bembenek, M. E., Hajipour, G., and Whitman, C. P. (1992) 4-Oxalocrotonate tautomerase, an enzyme composed of 62 amino acid residues per monomer, *J. Biol. Chem. 267*, 17716-17721.

18 Whitman, C. P., Aird, B. A., Gillespie, W. R., and Stolowich, N. J. (1991) Chemical and enzymatic ketonization of 2-hydroxymuconate, a conjugated enol, *J. Am. Chem. Soc. 113*, 3154-3162.

19 Wang, S. C., Johnson, W. H., Jr., Czerwinski, R. M., Stamps, S. L., Whitman, C. P. (2007) Kinetic and stereochemical analysis of YwhB, a 4-oxalocrotonate tautomerase homologue in *Bacillus subtilis*: mechanistic implications for the YwhB- and 4-oxalocrotonate tautomerase-catalyzed reactions, *Biochemistry 46*, 11919-11929.

20 Wang, S. C., Johnson, W. H., Jr., and Whitman, C. P. (2003) The 4-oxalocrotonate tautomerase- and YwhB-catalyzed hydration of 3*E*-haloacrylates: implications for evolution of new enzymatic activities, *J. Am. Chem. Soc. 125*, 14282-14283.

21 Poelarends, G. J., Serrano, H., Johnson, W. H., Jr., and Whitman, C. P. (2007) The phenylpyruvate tautomerase activity of *trans*-3-chloroacrylic acid dehalogenase: evidence for an enol intermediate in the dehalogenase reaction?, *Biochemistry 46*, 9596-9604.

22 Poelarends, G. J., Serrano, H., Person, M. D., Johnson, W. H., Jr., and Whitman, C. P. (2008) Characterization of Cg10062 from *Corynebacterium glutamicum*: implications for the evolution of *cis*-3-chloroacrylic acid dehalogenase activity in the tautomerase superfamily, *Biochemistry 47*, 8139-8147.

23 Afriat, L., Roodveldt, C., Manco, G., Tawfik, D. S. (2006) The latent promiscuity of newly identified microbial lactonases is linked to a recently diverged phosphotriesterase, *Biochemistry 45*,13677-13686.

24 Khersonsky, O., and Tawfik, D. S. (2010) Enzyme promiscuity: a mechanistic and evolutionary perspective, *Annu. Rev. Biochem. 79*, 471-505.

25 Wasiel, A. A., Rozeboom, H. J., Hauke, D., Baas, B. J., Zandvoort, E., Quax, W. J., Thunnissen, A.-M. W. H., and Poelarends, G. J. (2010) Structural and functional characterization of a macrophage migration inhibitory factor homologue from the marine cyanobacterium *Prochlorococcus marinus, Biochemistry 49*, 7572-7581.

26 Sambrook, J., Fritsch, E. F., and Maniatis, T. (1989) *Molecular Cloning: A Laboratory Manual*, 2nd Ed., Cold Spring Harbor Laboratory, Cold Spring Harbor, NY.

27 Waddell, W. J. (1956) A simple ultraviolet spectrophotometric method for the determination of protein, *J. Lab. Clin. Med. 48*, 311-314.

28 Zandvoort, E., Baas, B. J., Quax, W. J., and Poelarends, G. J. (2011) Systematic screening for catalytic promiscuity in 4-oxalocrotonate tautomerase: Enamine formation and aldolase activity, *ChemBioChem. 12, 602-609.*

29 Keuning, S., Janssen, D. B., and Whitholt, B. (1985) Purification and characterization of hydrolytic haloalkane dehalogenase from *Xanthobacter autotrophicus* GJ10, *J. Bacteriol. 163*, 635-639.

30 Johnson, W. H., Jr., Czerwinski, R. M., Fitzgerald, M. C., and Whitman, C. P. (1997) Inactivation of 4-oxalocrotonate tautomerase by 2-oxo-3-pentynoate, *Biochemistry 36*, 15724-15732.

31 Houmard, J., and Drapeau, G. R. (1972) Staphylococcal protease: a proteolytic enzyme specific for glutamoyl bonds, *Proc. Natl. Acad. Sci. U.S.A. 69*, 3506-3509.

32 Burks, E. A., Fleming, C. D., Mesecar, A. D., Whitman, C. P., Pegan, S. D. (2010) Kinetic and structural characterization of a heterohexamer 4-oxalocrotonate tautomerase from *Chloroflexus aurantiacus* J-10-fl: Implications for functional and structural diversity in the tautomerase superfamily, *Biochemistry 49*, 5016-5027.

33 Stivers, J. T., Abeygunawardana, C., Mildvan, A. S., Hajipour, G., Whitman, C. P., and Chen, L. H. (1996) Catalytic role of the amino-terminal proline in 4-oxalocrotonate tautomerase: affinity labeling and heteronuclear NMR studies, *Biochemistry 35*, 803-813.

34 Stivers, J. T., Abeygunawardana, C., Mildvan, A. S., Hajipour, G., and Whitman, C. P. (1996) 4-Oxalocrotonate tautomerase: pH dependences of catalysis and pK_a values of active site residues, *Biochemistry 35,* 814-823.

35 Czerwinski, R. M., Johnson, W. H., Jr., Whitman, C. P. (1997) Kinetic and structural effects of mutations of the catalytic amino-terminal proline in 4-oxalocrotonate tautomerase, *Biochemistry 36*, 14551-14560.

36 Horvat, C. M., and Wolfenden, R. V. (2005) A persistent pesticide residue and the unusual catalytic proficiency of a dehalogenating enzyme, *Proc. Natl. Acad. Sci. USA 102*, 16199-16202.

Supplementary information

The experimental procedures used for the construction, expression, overproduction, and purification of His-tagged MsCCH2 wild-type and MsCCH2-P1A mutant, and the ^{1}H NMR spectroscopic analysis of the reaction of MsCCH2 with *trans*-3-chloroacrylate (**2**) and *cis*-3-chloroacrylate (**3**) are provided below. In addition, the experimental procedures used for and results of the ^{1}H NMR spectroscopic analysis of the reaction of MsCCH2 with (*p*-hydroxyphenyl)enolpyruvate (**10**) and the mass spectral analysis of the products of the MsCCH2-catalyzed reaction with 2-oxo-3-pentynoate (**12**) are provided below.

Supplementary methods

Construction of the MsCCH2 Expression Vector. The gene coding for MsCCH2 was amplified using two synthetic primers, genomic DNA of *M*. *smegmatis* strain MC2 155, and the PCR reagents supplied in the Phusion DNA Polymerase system. The genomic DNA of strain MC2 155 (GenBank sequence: CP000480) was kindly provided by Professor William R. Jacobs, Jr. (Howard Hughes Medical Institute, Chevy Chase, MD). The forward primer 5'-A TAG CAG GTA **CAT ATG** CCC GTC TAC ACC GTC AC-3' contains an *Nde*I restriction site (in bold) followed by 17 bases corresponding to the coding sequence of the gene. To clone the gene for MsCCH2 in frame with the sequence that codes for the polyhistidine region of the expression vector pET20b(+), the reverse primer 5'-G TGA TGT TAT **AAG CTT** CCG AGA ACC TGA GCT CT-3' (primer R), which contains a *Hin*dIII restriction site (in bold), was used. The amplification mixture was made up in Phusion High-Fidelity buffer and contained 250 μM of each dNTP, 150 ng of each primer, 250 ng of total genomic DNA, and 1 U of Phusion DNA polymerase. The cycling parameters were 95 ^{o}C for 5 min followed by 35 cylces of 98 ^{o}C for 30 s, 45 ^{o}C for 30 s and 72 ^{o}C for 20 s, with a final elongation step of 72 ^{o}C for 10 min. The resulting PCR product and the pET-20b(+) vector (Novagen) were digested with *Nde*I and *Hin*dIII restriction enzymes, after which the vector was dephosphorylated with alkaline phosphatase. Following purification, the PCR product and vector were ligated using T4 DNA ligase. An aliquot of the ligation mixture was transformed into competent *Escherichia coli* BL21 (DE3) cells. Transformants were selected at 37 ^{o}C on LB/ampicillin plates. Plasmid DNA was isolated from several colonies and analyzed by restriction analysis for the presence of the insert. The cloned gene was sequenced to verify that no mutations had been introduced during the amplification of the gene. The newly constructed expression vector for MsCCH2 was named pMsCCH2.

Construction of the MsCCH2-P1A Mutant. The MsCCH2-P1A mutant was generated by PCR using plasmid pMsCCH2 as the template and primers F (5'-A TAG CAG GTC **CAT ATG** GCC GTC TAC ACC GTC AC-3') and R. Primer F contains an *Nde*I restriction site (in bold) and the mutated codon (underlined), followed by 14 bases corresponding to the coding sequence of the gene. The PCR product was generated and cloned into the pET-20b(+) vector as described above for the wild-type MsCCH2 encoding gene. The cloned mutant gene was completely sequenced to verify that only the intended mutation had been

introduced. The expression vector for the MsCCH2-P1A mutant was named pMsCCH2-P1A.

Expression and Purification of His-Tagged MsCCH2 Proteins. The MsCCH2 proteins, either wild-type or P1A mutant, were produced constitutively in *E. coli* BL21(DE3) using the T7 expression system. Fresh BL21(DE3) transformants containing the appropriate expression plasmid, either pMsCCH2 or pMsCCH2-P1A, were collected from a LB/ampicillin plate and used to inoculate LB/ampicillin medium (5 mL). After growth for 5 h at 37 ^{o}C, this culture was used to inoculate fresh LB/ampicillin medium (1 L) to a starting OD_{600} of about 0.01. After overnight growth at 30 ^{o}C with vigorous shaking, cells were harvested by centrifugation (10 min at 2300*g*) and resuspended in 10 mM NaH_2PO_4 buffer, pH 7.3 (buffer A), to a total volume of about 10 mL. Protease inhibitors (Complete Mini, Roche, Mannheim, Germany) were added and cells were disrupted by sonication for 5 × 1 min (with 5 min rest in between each cycle) at 50% duty cycle/50% output in a Branson Sonifier 450 (Branson Ultrasonics Corporation, Danbury, CT). Unbroken cells and debris were removed by centrifugation (45 min at 18000*g*). The supernatant was filtered through a 0.2 µm pore diameter filter, made 10 mM in imidazole (from a 1 M stock solution in water, pH adjusted to 7.3), and applied to a gravity flow column containing 0.5 mL Ni-Sepharose 6 Fast Flow resin. After overnight incubation at 4 ^{o}C, while mixing at 60 rpm on a rotor, the nonbound proteins were removed from the column by gravity flow. The column was washed with 40 mM imidazole in buffer A, after which retained proteins were eluted with 1 mL of 250 mM imidazole in buffer A. Subsequently, the protein sample was applied to a PD-10 gelfiltration column, which was previously equilibrated in buffer A, and proteins were eluted with buffer A. Fractions (1 mL) were analyzed by SDS-PAGE, and those containing highly purified MsCCH2 were combined and concentrated to a protein concentration of 5-20 mg/mL using a Vivaspin centrifugal concentrator equipped with a 5000 Da molecular weight cut-off filtration membrane (Sartorius Stedim Biotech S.A., France).

*^{1}H NMR Spectroscopic Analysis of the Reaction of MsCCH2 with p-Hydroxyphenylenolpyruvate (**10**)*. A series of ^{1}H NMR spectra monitoring the MsCCH2-catalyzed conversion of **10** to *p*-hydroxyphenylpyruvate (**11**) was recorded using a procedure described elsewhere (*1*) with the following modifications. An aliquot (550 µL) of a solution of **10** (50 µmol in 2 mL of 50 mM acetate buffer, pH 6.2) was added to an NMR tube containing D_2O (50 µL) and MsCCH2 (50 µL from a 5 mg/mL stock solution in 10 mM Na_2HPO_4 buffer, pH 7.3). The control sample for analyzing the nonenzymatic rate was prepared in the same way, but now 50 µL of 10 mM Na_2HPO_4 buffer (pH 7.3) was added to the NMR tube instead of 50 µL of MsCCH2. ^{1}H MNR spectra were recorded directly after mixing and then after 5, 10 and 15 min. The ^{1}H NMR signals for **10** and **11** are reported elsewhere (*1*).

*^{1}H NMR Spectroscopic Analysis of the Reaction of MsCCH2 with **2** and **3**.* A series of ^{1}H NMR spectra monitoring the MsCCH2-catalyzed dehalogenation of *trans*-3-chloroacrylate (**2**) or *cis*-3-chloroacrylate (**3**) was recorded according to protocols reported elsewhere (*2,3*) with the following modifications. An aliquot of MsCCH2 (50 µL from a 20 mg/mL stock solution in 10 mM Na_2HPO_4 buffer, pH 7.3) was added to an

NMR tube containing D_2O (50 µL) and 500 µL of a 60 mM solution of **2** or **3** in 100 mM Na_2HPO_4 buffer (pH adjusted to either 6.5 or 9.2). The first ^1H NMR spectrum was recorded directly after mixing, and then after 1 and 14 days. After 14 days of incubation at either pH 6.5 or pH 9.2, the spectrum for the mixture containing MsCCH2 and **2** exhibited signals corresponding to **2**, acetaldehyde, and the hydrate of acetaldehyde. The spectrum for the mixture containing MsCCH2 and **3** exhibited signals corresponding to **3**, acetaldehyde, and the hydrate of acetaldehyde (both at pH 6.5 and 9.2). The ^1H NMR signals for **2**, **3**, acetaldehyde, and the hydrate of acetaldehyde are reported elsewhere (*2,3,4*).

*Mass Spectral Analysis of the Product of the MsCCH2-Catalyzed Hydration of 2-Oxo-3-Pentynoate (**12**)*. To identify acetopyruvate (**13**) as the product of the MsCCH2-catalyzed hydration of **12** the following reactions were performed. An aliquot of MsCCH2 (from a 5 mg/mL stock solution in 5 mM NH_4HCO_3 buffer, pH 7.3) was diluted into 1 mL of 5 mM NH_4HCO_3 buffer (pH 6.8), yielding a final enzyme concentration of 62 µM. The reaction was initiated by the addition of 10 µL of **12** (from a 40 mM stock solution in 10 mM Na_2HPO_4 buffer, pH adjusted to 7.3), yielding a final substrate concentration of 400 µM. In a separate control reaction, CaaD (27 µM) was incubated with **12** (400 µM) under identical conditions to produce **13**, which was used as reference compound. The two reactions were monitored spectrophotometrically at 294 nm (λ_{max} of **13**) until completion, after which the enzyme was removed from each reaction mixture by centrifugation on vivaspin centrifugal concentrator equipped with a 2000 Da molecular weight cut-off filtration membrane. The flow-through of each reaction mixture was placed on ice and directly analyzed by ESI-MS and MS/MS.

Supplementary results

*MsCCH2-Catalyzes the Conversion of **10** to **11**.* The MsCCH2-catalyzed tautomerization of **10** was also monitored by ^1H NMR spectroscopy to verify that the reaction results in the formation of **11**. The spectrum recorded immediately after dissolving *p*-hydroxyphenylpyruvate in acetate buffer revealed two doublets in the aromatic region (7.53 and 6.78 ppm) and a singlet representing an olefinic proton at 6.20 ppm. These signals are consistent with the enol form of the substrate. The MsCCH2-catalyzed conversion of the enol form yields the keto form, as indicated by changes in the chemical shifts of the aromatic protons (to 7.00 and 6.75 ppm) and the appearance of a singlet at 3.87 ppm, which corresponds to the methylene protons. After a 10 min-incubation period, the ratio of keto:enol is ~5 (Figure S1A). For comparison, a 10 min-incubation period in the absence of enzyme yields a keto:enol ratio of ~0.12 (Figure S1B). These observations confirm that **11** is the product of the MsCCH2-catalyzed conversion of **10**.

*MsCCH2-Catalyzes the Conversion of **12** to **13** and **14**.* While **13** has a characteristic λ_{max} of 294 nm (*2*), its formation in the reaction of **12** with MsCCH2 was confirmed by ESI-MS and MS/MS analyses. Accordingly, MsCCH2 was incubated with **12** in 5 mM NH_4HCO_3 buffer (pH 6.8). In a separate control reaction, CaaD was incubated with **12** under identical conditions to produce **13**, which was used as reference compound. The two

reactions were monitored spectrophotometrically at 294 nm until completion, after which the enzymes were removed from the reaction mixtures by centrifugation on vivaspin concentrators. The flow-through of each reaction mixture was analyzed by ESI-MS. The spectrum revealed a major product for the MsCCH2-catalyzed reaction with a mass (129.2 Da) nearly identical to that found for the product of the CaaD-catalyzed reaction (129.1 Da). MS/MS analysis of the precursor ion of the 129.2 Da product of the MsCCH2-catalyzed reaction revealed fragment ions with masses (44.9, 57.0, and 84.9 Da) identical to those found with the 129.1 Da product of the CaaD-catalyzed reaction. Based on these results, we conclude that **13** is indeed the product of the MsCCH2-catalyzed hydration of **12**.

We next investigated whether the absorbance peak at 324 nm corresponds to the covalent modification of MsCCH2 by **12**, presumably yielding enamine species **14**. Accordingly, MsCCH2 was treated with **12** at pH 7.3, after which the enzyme was separated from the free substrate (**12**) and product (**13**) by centrifugation on a vivaspin column. Analysis of the purified enzyme by UV spectroscopy demonstrated that the absorbance at 324 nm is indeed associated with a covalent adduct on the enzyme rather than an unbound reaction product.

MsCCH2 was also treated with **12** at pH 7.3 and directly analyzed by ESI-MS. The reconstruct of the ESI mass spectrum revealed two major peaks, one corresponding to the mass of unmodified MsCCH2 (16092 Da) and the other to the mass expected for modified MsCCH2 (16204 Da). Hence, the difference between the masses is 112 Da, consistent with covalent modification of the enzyme by a single molecule of **12** (*5*). A comparison of the signal intensities in the ESI mass spectrum suggests that about 30% of the enzyme is covalently modified by **12**.

Supplementary figures

Figure S1A

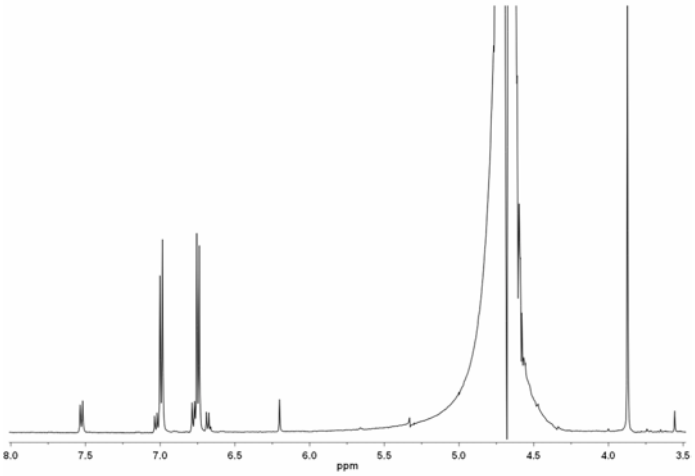

Figure S1B

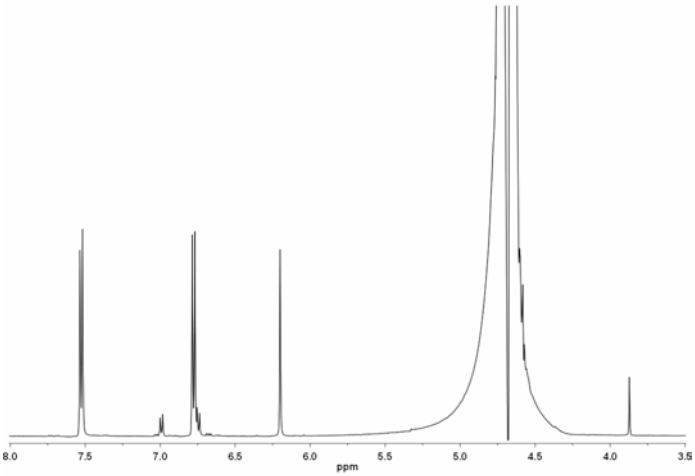

Figure S1. ^{1}H NMR spectra monitoring the conversion of *p*-hydroxyphenylenolpyruvate (**10**) to *p*-hydroxyphenylpyruvate (**11**). (A) Spectrum of the MsCCH2-catalyzed conversion of **10** to **11**. (B) Spectrum of the non-enzymatic conversion of **10** to **11**. Both spectra were recorded 10 min after the addition of **10** to the reaction mixture. The ^{1}H NMR signals for compounds **10** and **11** are reported elsewhere (*1*).

Supplementary references

1 Wasiel, A. A., Rozeboom, H. J., Hauke, D., Baas, B. J., Zandvoort, E., Quax, W. J., Thunnissen, A.-M. W. H., and Poelarends, G. J. (2010) Structural and functional characterization of a macrophage migration inhibitory factor homologue from the marine cyanobacterium *Prochlorococcus marinus, Biochemistry 49*, 7572-7581.

2 Wang, S. C., Person, M. D., Johnson, W. H., Jr., and Whitman, C. P. (2003) Reactions of *trans*-3-chloroacrylic acid dehalogenase with acetylene substrates: Consequences of and evidence for a hydration reaction, *Biochemistry 42*, 8762–8773.

3 Poelarends, G. J., Serrano, H., Person, M. D., Johnson, W. H., Jr., Murzin, A. G., and Whitman, C. P. (2004) Cloning, expression, and characterization of a *cis*-3-chloroacrylic acid dehalogenase: Insights into the mechanistic, structural, and evolutionary relationship between isomer-specific 3-chloroacrylic acid dehalogenases, *Biochemistry 43*, 759–772.

4 Wang, S. C., Johnson, W. H., Jr., and Whitman, C. P. (2003) The 4-oxalocrotonate tautomerase- and YwhB-catalyzed hydration of 3*E*-haloacrylates: implications for evolution of new enzymatic activities, *J. Am. Chem. Soc. 125*, 14282-14283.

5 Johnson, W. H., Jr., Czerwinski, R. M., Fitzgerald, M. C., and Whitman, C. P. (1997) Inactivation of 4-oxalocrotonate tautomerase by 2-oxo-3-pentynoate, *Biochemistry 36*, 15724-15732.